

Infrared Satellite Retrievals in the Presence of Stratospheric Aerosol

CHRISTOPHER J. MERCHANT AND MARK A. SAUNDERS

Department of Space and Climate Physics, Mullard Space Science Laboratory, Dorking, Surrey, United Kingdom

14 January 1997 and 22 September 1997

ABSTRACT

The presence of stratospheric aerosol can bias the results of infrared satellite retrievals of sea surface temperature (SST) and total precipitable water (TPW). In the case of linear SST retrieval using the Along Track Scanning Radiometer (ATSR), on the ESA European remote-sensing satellites, constant coefficients can be found that give negligible bias (less than 0.1 K) over a wide range of aerosol amount (11- μm optical thickness from 0.0 to 0.022). For TPW retrieval, in contrast, the biases associated with stratospheric aerosol are less satisfactory (2 kg m⁻² or greater across a range of 11- μm optical thickness of 0.0–0.01). However, the authors show how to find optimal aerosol-dependent retrieval coefficients for any stratospheric aerosol distribution from knowledge of the mean and variance of that aerosol distribution. Examples of SST and TPW retrieval using simulated ATSR brightness temperature data are given.

1. Introduction

Data products such as sea surface temperature (SST) generated from the observations of infrared radiometers on satellites are known to be prone to bias when significant amounts of aerosol are present in the stratosphere (e.g., Reynolds 1993). Brown et al. (1997) have shown that the dual-view capability of the Along Track Scanning Radiometer (ATSR) allows linear SST algorithms to be made “robust” against the effects of stratospheric aerosol (hereafter referred to simply as “aerosol”) and that one set of robust coefficients can be applied across a wide range of aerosol concentrations with negligible bias in the SST retrieval.

This note develops the theory underlying the generation of aerosol-robust linear algorithms and shows how to assess the range of application of such algorithms. In the case of the retrieval using ATSR of total precipitable water (TPW), we find that the use of just one set of robust coefficients is not sufficient to render bias from aerosol negligible. However, we show that the calculations used to derive coefficients for the case where aerosol amounts are negligible can be readily adapted to apply to any aerosol distribution, without the usual need for extensive radiative transfer calculations and regression analysis.

2. Theory of aerosol-robust linear algorithms

In this section, we derive two useful results: 1) a means of assessing the retrieval bias caused by aerosol when using a set of constant coefficients and 2) a formula by which optimal aerosol-dependent coefficients can be derived without recalculation of the full problem. The aerosol-dependent coefficients we derive are optimal in the sense that, for a given aerosol distribution, they are unbiased and give the minimum retrieval error.

Estimates of SST are derived from satellite infrared brightness temperatures using linear algorithms (see, e.g., Zavody et al. 1995) of the following form:

$$x_r = a_0 + \sum_{\text{channels } i} a_i y_i = a_0 + \mathbf{a}^T \mathbf{y}, \quad (1)$$

where a_0 and a_i are constant coefficients and y_i is the i th brightness temperature. The variable x_r is then the estimate of SST, but other quantities, such as TPW, may be derived using the same form with appropriate coefficients. The rightmost part of (1) expresses the algorithm in the form of the inner product of the column vectors \mathbf{a} and \mathbf{y} , whose elements are a_i and y_i , respectively. (Throughout, the superscript T indicates the transpose, bold roman type is used for column vectors, and bold sans serif is for matrices.)

The coefficients a_0 and \mathbf{a} are usually derived by ordinary least squares regression on a set of known values of \mathbf{y} and x_r , the known values being either experimental or computed. The standard expression for the coefficients is

$$\begin{aligned} \mathbf{a} &= (\mathbf{y}\mathbf{y}^T - \bar{\mathbf{y}}\bar{\mathbf{y}}^T)^{-1}(\bar{x}_r\bar{\mathbf{y}} - \bar{x}_r\bar{\mathbf{y}}) \\ a_0 &= \bar{x}_r - \mathbf{a}^T\bar{\mathbf{y}}, \end{aligned} \quad (2)$$

Corresponding author address: Christopher J. Merchant, Department of Space and Climate Physics, University College London, Mullard Space Science Laboratory, Holmbury St. Mary, Dorking, Surrey RH5 6NT, United Kingdom.
E-mail: cjm@mssl.ucl.ac.uk

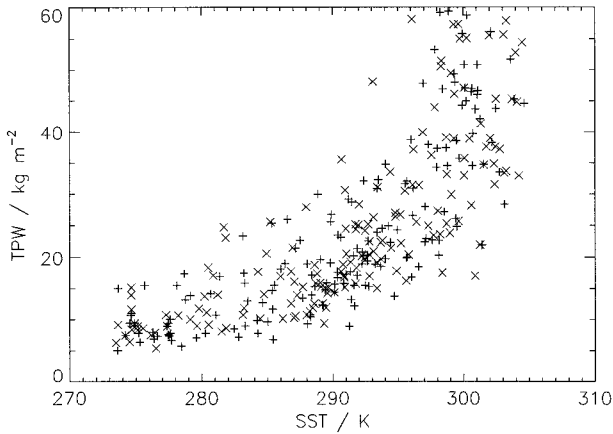


FIG. 1. Distribution of SST and TPW in the 332 profiles used in this study. SST and TPW are the principal factors governing infrared brightness temperatures. Points are marked (+) or (x) according to whether the profile was allocated to set 1 or 2, respectively (see text).

where a bar over a quantity indicates the average and the inverse is a matrix inverse.

Let the atmospheric and sea surface state be adequately described (for the purposes of determining the top-of-atmosphere brightness temperatures) by a vector,

$$\mathbf{x} = \begin{bmatrix} \mathbf{x}_0 \\ x_{SA} \end{bmatrix}, \quad (3)$$

where the element describing the optical thickness of aerosol x_{SA} has been distinguished from the remaining elements, denoted \mathbf{x}_0 . The quantity that it is required to retrieve from the satellite observations using a linear algorithm, x_r , is a function of the elements of \mathbf{x}_0 .

Let the satellite observations be $\mathbf{y} = F(\mathbf{x}_0; x_{SA}) + \varepsilon$, where the function F gives in terms of the state vector the true brightness temperature of the top-of-atmosphere fluxes integrated across the the radiometer channels, and ε represents instrumental errors.

Make the following assumptions.

- 1) It is a good approximation to write

$$F(\mathbf{x}_0; x_{SA}) = F(\mathbf{x}_0; 0) + x_{SA}\mathbf{k} = \mathbf{y}_0 + x_{SA}\mathbf{k}, \quad (4)$$

where $\mathbf{k} = \overline{\partial\mathbf{y}/\partial x_{SA}}$, the mean of the partial derivative of the observation vector with respect to x_{SA} . This says that the presence of aerosol changes the brightness temperatures by an amount proportional to the aerosol amount, and that $\partial\mathbf{y}/\partial x_{SA}$ is at most a weak function of any element of \mathbf{x} ; \mathbf{y}_0 is the satellite ob-

servations in the absence of aerosol and instrumental noise.

- 2) Here, x_{SA} is uncorrelated with every element of x_0 .
- 3) Instrumental noise ε is zero mean with covariance matrix \mathbf{S}_ε and is uncorrelated with \mathbf{y}_0 or x_{SA} .

Granted these assumptions, (2) becomes

$$\begin{aligned} \begin{bmatrix} \mathbf{a} \\ a_0 \end{bmatrix} &= \begin{bmatrix} (\overline{\mathbf{y}_0\mathbf{y}_0^T} + \mathbf{S}_\varepsilon + \nu\mathbf{k}\mathbf{k}^T) & (\overline{\mathbf{y}_0} + \mu\mathbf{k}) \\ (\overline{\mathbf{y}_0} + \mu\mathbf{k})^T & 1 \end{bmatrix}^{-1} \\ &\quad \times \begin{bmatrix} \overline{x_r\mathbf{y}_0} + \overline{x_r}\mu\mathbf{k} \\ \overline{x_r} \end{bmatrix} \\ &= (\mathbf{M}_0 + \mathbf{M}_{SA})^{-1}(\mathbf{b}_0 + \mathbf{b}_{SA}), \end{aligned} \quad (5)$$

where

$$\begin{aligned} \mathbf{M}_0 &= \begin{bmatrix} \overline{\mathbf{y}_0\mathbf{y}_0^T} + \mathbf{S}_\varepsilon & \overline{\mathbf{y}_0} \\ \overline{\mathbf{y}_0}^T & 1 \end{bmatrix}, \\ \mathbf{M}_{SA} &= \nu \begin{bmatrix} \mathbf{k}\mathbf{k}^T & 0 \\ 0 & 0 \end{bmatrix} + \mu \begin{bmatrix} 0 & \mathbf{k} \\ \mathbf{k}^T & 0 \end{bmatrix}, \\ \mathbf{b}_0 &= \begin{bmatrix} \overline{x_r\mathbf{y}_0} \\ \overline{x_r} \end{bmatrix}, \\ \mathbf{b}_{SA} &= \mu \begin{bmatrix} \overline{x_r}\mathbf{k} \\ 0 \end{bmatrix}, \\ \mu &= \overline{x_{SA}}, \end{aligned}$$

and

$$\nu = \overline{x_{SA}^2}.$$

In (5) we have separated out the effect of aerosol on the optimal coefficients. In the case of negligible aerosol amount, the coefficients are found from \mathbf{M}_0 and \mathbf{b}_0 , both of which may be calculated once only and kept, along with $\overline{x_r}$. The vector \mathbf{k} can also be precalculated. Thereafter, to derive optimal coefficients for the case where aerosol is present, the only recalculation required is to include \mathbf{M}_{SA} and \mathbf{b}_{SA} , which vary with μ (the mean aerosol amount) and ν (the variance of the aerosol amount) only.

Consider applying coefficients \mathbf{a} , found from (5) with $\overline{x_{SA}} = \mu_1$ and $\overline{x_{SA}^2} = \nu_1$, to observations in circumstances in which the distribution of aerosol is described by μ_2 and ν_2 . The bias of the retrievals is

$$\mathbf{a}^T\mathbf{k}(\mu_1 - \mu_2). \quad (6)$$

Thus, if the acceptable bias in the retrieval is $\pm\delta$, the coefficients \mathbf{a} can be applied so long as $|\mu_1 - \mu_2| < |\delta/\mathbf{a}^T\mathbf{k}|$. This, then, gives us a means of assessing the range of aerosol distributions over which a particular robust algorithm can be applied.

TABLE 1. Infrared optical thickness (IROT) and brightness temperature noise (rms).

Channel	IROT (nadir, scaling = 1.0)	Noise
3.7 μm	0.012	0.05 K
11 μm	0.010	0.04 K
12 μm	0.008	0.05 K

TABLE 2. Coefficients for dual-view three-channel retrieval algorithms. Here “3.7 *n*” indicates the coefficient multiplying the brightness temperature of the 3.7- μm channel in nadir view, etc. These algorithms apply to brightness temperature (K).

Description	a_0	\mathbf{a}					
		3.7 <i>n</i>	3.7 <i>f</i>	11 <i>n</i>	11 <i>f</i>	12 <i>n</i>	12 <i>f</i>
SST							
Aerosol-robust	-2.29	1.30435	-0.27228	0.44891	-0.41638	0.03864	-0.09293
TPW							
From (5) with $\mu = 0.5, \nu = 0.417$	-38.0	-0.260	8.193	-0.106	3.689	-14.476	3.199

3. Example 1: SST retrieval using ATSR (dual view)

The ATSR detects radiation in channels nominally at wavelengths of 3.7, 11, and 12 μm at two look angles: nadir and forward (0° and approximately 55° from vertical at the center of swath, respectively). A given area of sea surface is first viewed in forward look and then in nadir look a few minutes later. The ATSR swath width is approximately 500 km, and the finest image resolution is 1 km^2 . [For descriptions of the ATSR instrument and its SST retrieval capability see, e.g., Edwards et al. (1990) and Harris and Saunders (1996).]

We consider center-swath dual-view three-channel SST algorithms. Such algorithms are a weighted sum of six brightness temperatures plus an offset. To derive the results presented in this and the next section, we use a global set of 332 radiosonde profiles of the atmospheric column (temperature, pressure, and humidity) and associated brightness temperatures, as calculated by a modified version of the ATSR-specific radiative transfer code, RADGEN (Zavody et al. 1995). [The modifications include a change to the sea surface emissivity parameterization to that of Watts et al. (1996).] The 332 profiles cover all latitudes and seasons, and their distribution of SST and TPW is shown in Fig 1. For each profile, we calculate brightness temperatures for 27 different combinations of three other quantities: air-sea temperature difference (surface air minus sea surface temperature equal to -3.0, -0.5, 2.0 K), wind speed (0, 5, 15 m s^{-1}), and stratospheric aerosol amount. The stratospheric aerosol amount is here described by a dimensionless factor that scales the infrared optical thickness of aerosol for the three channels. An aerosol scale factor of 1.0 indicates channel-integrated optical thicknesses as given in Table 1 and represents aerosol typically present up to a year after a major volcanic eruption,

such as that of Mount Pinatubo in 1991 (Lambert et al. 1993). The ratios of aerosol extinction to scattering cross section assumed are those chosen by Zavody et al. (1995) to represent aged volcanic aerosols. We use aerosol scale factors of 0.0, 0.5, and 1.0.

From the calculated brightness temperatures, we find that the effects of air-sea temperature difference and wind speed on brightness temperatures are nonlinear. Variations in these two quantities are simply included in the data used to find \mathbf{M}_0 and \mathbf{b}_0 . In contrast, the effect of aerosol on brightness temperature is linear, that is, assumption 1 (section 2) is found to be reasonable for aerosol with

$$\mathbf{k} = (-0.256, -0.445, -0.496, -0.849, -0.382, -0.650),$$

where the elements refer to the gradient of brightness temperature with respect to an aerosol scaling factor for 3.7- μm nadir, 3.7- μm forward, 11- μm nadir, 11- μm forward, 12- μm nadir, and 12- μm forward, respectively. Here, \mathbf{k} is the mean overall profiles of $[\mathbf{y}(\mu_2) - \mathbf{y}(\mu_1)]/(\mu_2 - \mu_1)$, where the subscripts 1 and 2 refer to any pair of the three aerosol-scale factors referred to above. The largest standard error in any of the elements in \mathbf{k} given above is 0.002.

Assumption 2 is certainly valid on scales of the order of the ATSR swath width. On a global scale, however, aerosol amount and SST may by chance be correlated after, for example, a volcanic eruption near the equator, because both will have a dependence on latitude.

Assumption 3 is approximately valid for ATSR; in this study we use brightness temperature noise as given in Table 1 and take the matrix \mathbf{S}_e to be diagonal (noise uncorrelated between channels). These numbers are based on current performance of ATSR-2 (A. M. Zavody 1996, personal communication) but would also adequately represent the brightness temperature noise of ATSR-1 a year after the Pinatubo eruption (Harris and Saunders 1996).

The coefficients for a robust dual-view three-channel algorithm, found using (5) with $\mu = 0.5$ and $\nu = 0.417$ (values corresponding to the inclusion of aerosol at 0.0, 0.5, and 1.0 scaling factor), are given in Table 2. (The ordering of the elements of \mathbf{a} is the same as that of \mathbf{k} above.) The root-mean-square (rms) error in SST retrieval for this algorithm (when applied back to the sim-

TABLE 3. Characteristics of data subsets used in examples 2 and 3.

Label	Aerosol amounts included	μ	
		μ	ν
A1 and A2	0.0	0.0	0.0
B1 and B2	0.0, 0.5	0.25	0.125
C1 and B2	0.0, 0.5, 1.0	0.5	0.417
D1 and D2	0.5, 1.0	0.75	0.625

TABLE 4. Performance of three-channel dual-view retrieval algorithms for TPW. Here “A1” means an algorithm derived by full regression of TPW against brightness temperatures in data subset A1 (see Table 3), etc., and “Eq. (5)” means found from (5).

Basis of algorithm	Measure	Applied to data subset			
		A2	B2	C2	D2
A1	rms error/kg m ⁻²	4.5	8.2	13.1	15.8
B1		5.4	5.4	6.3	6.6
C1		5.8	5.6	5.7	5.7
D1		7.7	6.6	6.3	5.4
Eq. (5)		4.5	5.4	5.7	5.4
A1	Bias/kg m ⁻²	0.0	5.0	9.9	14.8
B1		-1.9	0.0	1.9	3.8
C1		-1.9	-0.9	0.0	1.0
D1		-5.8	-3.8	-1.9	0.0
Eq. (5)		0.0	0.0	0.0	0.0

ulated observations plus simulated brightness temperature noise) is 0.1 K.

Assuming 0.1 K is also the acceptable retrieval bias from aerosol, the range of μ over which these coefficients may be applied is, from (6), 0.0–2.2. The observation of Brown et al. (1997) that an aerosol-robust SST algorithm has low bias over a range of aerosol distributions is confirmed and shown to be a result of the smallness of $\mathbf{a}^T \mathbf{k}$.

4. Example 2: TPW retrieval using ATSR

For the same set of atmospheric profiles, we investigate the retrieval of TPW using ATSR. We randomly divide the profiles in two sets of 166 profiles: the first (labeled 1) to be used to derive retrieval algorithms, and the second (labeled 2) to act as independent data for assessing the performance of the algorithms. In Fig. 1, points are marked with (+) for set 1 and (×) for set 2. Four retrieval algorithms (labeled A–D) are found by full regression of TPW against calculated brightness temperatures for various subsets of the simulated data in set 1. All four subsets include all variations in air–sea temperature difference and wind speed (nine combinations for each profile), but different combinations of aerosol amount are included in each, as shown in the second column of Table 3. In addition, we find the optimum robust algorithm for each aerosol combination using (5) with the values for μ and ν shown in Table 3. For reference, the algorithm from (5) for the widest aerosol variation (subset C1) is listed in Table 2.

Table 4 shows the results of applying each algorithm to all four aerosol distributions, as before with simulated noise added to the brightness temperatures. The performance of the retrieval using optimum coefficients derived from (5) in each case matches that of the best set of coefficients found by full regression analysis of TPW and brightness temperatures in terms of both rms error and bias (always zero). The biases in TPW retrieval from applying the nonoptimum “robust” algorithms to other data subsets are of the order

of 2 kg m⁻² (typically 4%–10% of TPW) and would be larger with more extreme aerosol variations present.

Robust TPW algorithms are therefore seen to suffer significant bias when (mis)applied to a wide range of aerosol distributions. (Of course, nonrobust algorithms yield retrievals with even greater biases when similarly used.) For TPW algorithms, \mathbf{a} is not rendered sufficiently orthogonal to \mathbf{k} . This may be because the effects of increasing aerosol amount and increasing TPW on brightness temperatures are similar in that “forward” brightness temperatures are, in both cases, lowered about twice as much as “nadir” brightness temperatures because of the longer path-length through the atmosphere in forward view.

Optimum TPW retrievals can therefore only be achieved by taking account of the distribution of aerosols present. We find, in fact, that aerosol amount itself can be retrieved using a three-channel dual-view algorithm that turns out to be robust to variations in TPW. The point rms error in retrieved scaling factor is 0.2, which is adequate for deriving good estimates of the mean and mean-square aerosol amounts (μ and ν) over a field of view. Otherwise, independent measures of μ and ν can be used. Coefficients for the optimum retrieval of TPW in that same field of view then follow by application of (5).

5. Example 3: Single-view SST retrieval

Table 5 shows the results of following the procedure of example 2, but applied to SST retrieval using nadir brightness temperatures only. The single-view algorithms generated by regression are not fully robust, giving residual biases of the order of 0.2 K when applied to other distributions of aerosol. Again, use of (5) allows such biases to be eliminated and the root-mean-square retrieval error to be reduced to 0.15 K or less.

Also in Table 5 is the performance of a single-view algorithm of form $a_0 + a_1 T_{12} + a_2 (T_{3.7} - T_{11})$, labeled R. (Here, $T_{3.7}$ is the nadir brightness temperature in

TABLE 5. Performance of single-view SST algorithms. Nomenclature as Table 4 but with "R" indicating use of the form reported by Reynolds (1993).

Basis of algorithm	Measure	Applied to data subset			
		A2	B2	C2	D2
A1	rms error/K	0.10	0.15	0.23	0.27
B1		0.13	0.13	0.17	0.19
C1		0.18	0.15	0.15	0.14
D1		0.24	0.19	0.17	0.13
Eq. (5)		0.10	0.13	0.15	0.13
R		0.59	0.58	0.58	0.58
A1	Bias/K	0.00	0.08	0.16	0.24
B1		-0.07	0.00	0.07	0.15
C1		-0.14	-0.07	0.00	0.07
D1		-0.21	-0.14	-0.07	0.00
Eq. (5)		0.00	0.00	0.00	0.00
R		-0.05	-0.02	0.00	0.03

the 3.7- μm channel, and so on.) This is the form (at center swath) reported by Reynolds (1993) and used after the Pinatubo eruption for retrievals of SST from the Advanced Very High Resolution Radiometer (AVHRR). AVHRR is a single-view instrument (on board the NOAA series of polar-orbiting satellites), which includes channels spectrally equivalent to the infrared channels of ATSR. We found the coefficients for R using the data subset C1. This form is, as stated by Reynolds (1993), robust to changing distributions of aerosol, as shown by the low biases of the R algorithm (0.05 K or less) in Table 5. The rms retrieval error of 0.6 K, however, is comparatively poor because an algorithm of this form is unable to deal as effectively with variations in TPW.

The AVHRR channel at 0.55 μm has been used to measure aerosol optical thickness using reflected sunlight (Stowe et al. 1992), and Baran and Foot (1994) have used the High-Resolution Infrared Radiation Sounder (on board the same series of satellites) to develop a climatology of the Pinatubo aerosol. It seems, then, that AVHRR SST retrieval accuracy could, in principle, be improved by using aerosol information available from other channels or instruments to form estimates of μ and ν and calculating the corresponding optimum SST coefficients.

6. Conclusions

We have seen that the effects of the presence of stratospheric aerosol on linear retrievals (bias and increased scatter) can be minimized by adapting the zero-aerosol retrieval coefficients using a simple computation, as described by (5). The results of retrievals found using (5) are bias free and have minimum scatter.

In the case of three-channel dual-view SST retrieval using ATSR, we have seen that such efforts are not usually necessary because SST retrieval coefficients can readily be made orthogonal to the mode of variation of brightness temperature introduced by strato-

spheric aerosol. Thus, one robust algorithm is adequate for all practical aerosol distributions.

In contrast, TPW retrieval using an algorithm with constant coefficients gives a less satisfactory degree of bias when aerosol is present. The use of (5) allows the straightforward calculation of the set of aerosol-dependent coefficients giving the optimum TPW retrieval in terms of the mean and mean-square aerosol amount. For the case of ATSR, these descriptors of the aerosol may be directly retrievable; otherwise, independent estimates could be used. We have applied this method of varying coefficients to retrieval of TPW from ATSR observations in numerical simulation, with encouraging results (Table 4). If shown to work in practice, this method will allow bias-free three-channel dual-view ATSR retrievals of TPW.

Our method can be used for three-channel single-view ATSR or AVHRR retrievals of SST, given independent knowledge of the mean and mean-square aerosol amount. In the case of AVHRR in particular, other channels or other instruments on the same satellite may provide that information. This could markedly improve the AVHRR SST retrieval accuracy (Table 5).

The formal technique may have applications to other observing systems.

Acknowledgments. We wish to thank Andrew Harris, David Pick, and Albin Zavody for fruitful discussions, and the anonymous reviewers for their comments. Chris Merchant is funded by NERC student-ship GT4/95/210/D, a CASE award with the U.K. Meteorological Office.

REFERENCES

- Baran, A. J., and J. S. Foot, 1994: New application of the operational sounder HIRS in determining a climatology of sulphuric acid aerosol from the Pinatubo eruption. *J. Geophys. Res.*, **99**, 25 673–25 679.
- Brown, S. J., A. R. Harris, I. M. Mason, and A. M. Zavody, 1997: New aerosol-robust sea surface temperature algorithms for

- ATSR, the Along Track Scanning Radiometer. *J. Geophys. Res.*, **102**, 27 973–27 989.
- Edwards, T., and Coauthors, 1990: The along-track scanning radiometer—Measurement of sea-surface temperature from *ERS-1*. *J. Bri. Interplanet. Soc.*, **43**, 160–180.
- Harris, A. R., and M. A. Saunders, 1996: Global validation of the along-track scanning radiometer against drifting buoys. *J. Geophys. Res.*, **101**, 12 127–12 140.
- Lambert, A., R. G. Grainger, J. J. Remedios, C. D. Rodgers, M. Corney, and F. W. Taylor, 1993: Measurements of the evolution of the Mt. Pinatubo aerosol cloud by ISAMS. *Geophys. Res. Lett.*, **20**, 1287–1290.
- Reynolds, R. W., 1993: Impact of Mount Pinatubo aerosols on satellite derived sea surface temperature. *J. Climate*, **6**, 768–774.
- Stowe, L., R. M. Carey, and P. P. Pellegrino, 1992: Monitoring the Mt. Pinatubo aerosol layer with *NOAA-11* AVHRR data. *Geophys. Res. Lett.*, **19**, 159–162.
- Watts, P. D., M. R. Allen, and T. J. Nightingale, 1996: Wind speed effects on sea surface emission and relection for the Along Track Scanning Radiometer. *J. Atmos. Oceanic Technol.*, **13**, 126–141.
- Zavody, A. M., C. T. Mutlow, and D. T. Llewellyn-Jones, 1995: A radiative transfer model for sea surface temperature retrieval for the along-track scanning radiometer. *J. Geophys. Res.*, **100**, 937–952.